Electrochemistry Communications 122 (2021) 106890

Contents lists available at ScienceDirect

Electrochemistry Communications

journal homepage: www.elsevier.com/locate/elecom

Dip-coating of MXene and transition metal dichalcogenides on 3D-printed nanocarbon electrodes for the hydrogen evolution reaction

K.P. Akshay Kumar [a], Kalyan Ghosh [a], Osamah Alduhaish [b,2], Martin Pumera [a,b,c,d,1,*]

[a] Future Energy and Innovation Laboratory, Central European Institute of Technology, Brno University of Technology, Purkyňova 123, 61200 Brno, Czech Republic
[b] Chemistry Department P.O. Box 2455, College of Science King Saud University, Riyadh 11451, Saudi Arabia
[c] Department of Chemistry and Biochemistry, Mendel University in Brno, Zemedelska 1, CZ-613 00, Brno, Czech Republic
[d] Department of Medical Research, China Medical University Hospital, China Medical University, No. 91 Hsueh-Shih Road, Taichung 40402, Taiwan

ARTICLE INFO

Keywords:
Fused deposition modeling
Dip-coating
MXene
TMDs
Hydrogen evolution reaction

ABSTRACT

3D-printing technology is widely accepted as a scalable and advanced manufacturing procedure for the fabrication of electrodes for electrochemical applications. 3D-printed carbon-based electrodes can be used for electrochemical analysis, replacing conventional carbon electrodes. However, a bare 3D-printed carbon electrode exhibits poor electrochemical performance. Herein, a post-treatment of 3D-printed electrodes was carried out using catalytically active materials to improve their electrochemical performance. We used a dip-coating technique which is a more universal, facile, and cost-effective approach compared with other conventionally used techniques such as atomic layer deposition or electrodeposition. The 3D-printed nanocarbon electrodes were dip-coated with MXene ($Ti_3C_2T_x$) and different transition metal dichalcogenides such as MoS_2, $MoSe_2$, WS_2, and WSe_2 to study their catalytic activity towards the hydrogen evolution reaction (HER). This study demonstrates a simple method of improving the catalytic surface properties of 3D-printed nanocarbon electrodes for energy conversion applications.

1. Introduction

3D-printing or additive manufacturing is attracting significant attention because it facilitates customized fabrication and rapid prototyping with high accuracy [1,2]. Fused deposition modeling (FDM) or fused filament modeling (FFM) is a 3D-printing approach in which thermoplastic filaments are extruded down the nozzle to print structures in a layer-by-layer manner [3,4]. Recently, a commercial conductive nanocarbon/polylactic acid (PLA) filament has been widely used for FDM 3D-printing and then for electrochemical applications [5–7]. The carbon surface of 3D-printed electrodes possesses poor electrocatalytic properties. Several methods of depositing catalysts over 3D-printed electrodes have been developed, including atomic layer deposition (ALD) [8], electrodeposition [9] and spray coating [10]. ALD requires specialized and expensive equipment, and is not suitable for rapid, low-cost manufacturing of 3D-printed electrodes. In addition, precursors for ALD deposition are limited, and thus not all required materials can be deposited on ALD electrodes. Electrodeposition of catalysts again requires precursor materials [9], which in many cases are not available. We thus turned to a proven technique of modifying surfaces with any electrocatalytic material, which is dip-coating [11,12].

Herein, we report the facile, cost-effective, binder-free dip-coating of a 3D-printed nanocarbon electrode in a slurry of MXene ($Ti_3C_2T_x$) and transition metal dichalcogenides (MoS_2, $MoSe_2$, WS_2, and WSe_2) for the hydrogen evolution reaction (HER). The modified electrodes are characterized by scanning electron microscopy (SEM), energy dispersive X-ray (EDX) spectroscopy, and the electrocatalytic activity of the dip-coated 3D-printed nanocarbon electrodes is assessed *via* linear sweep voltammetry (LSV) and chronoamperometry measurements. This dip-coating of electrocatalytic active materials over 3D-printed nanocarbon electrodes represents a simple and user-friendly approach towards energy conversion applications.

* Corresponding author at: Future Energy and Innovation Laboratory, Central European Institute of Technology, Brno University of Technology, Purkyňova 123, 61200 Brno, Czech Republic.
E-mail addresses: oalduhaish@ksu.edu.sa (O. Alduhaish), pumera.research@gmail.com (M. Pumera).
[1] Orcid: 0000-0001-5846-2951.
[2] Orcid: 0000-0001-5344-9459.

https://doi.org/10.1016/j.elecom.2020.106890
Received 5 November 2020; Received in revised form 24 November 2020; Accepted 25 November 2020
Available online 2 December 2020

2. Experimental section

2.1. Materials and methods

N,*N*-Dimethylformamide (DMF), ethanol, sulfuric acid (H_2SO_4), molybdenum sulfide (MoS_2), molybdenum selenide ($MoSe_2$), tungsten sulfide (WS_2), and tungsten selenide (WSe_2) were purchased from Sigma-Aldrich, Germany. MXene (Ti_3C_2) ceramic aqueous paste was purchased from Y-carbon, Ukraine. All chemicals were of analytical grade and used as received. The conductive graphene/polylactic acid (PLA) filament was procured from Graphene Laboratories Inc., New York, USA.

2.2. Preparation of 3D-printed electrodes

The electrodes were designed using Autodesk Fusion 360 software and then printed using a Prusa i3 MK3s printer (Prusa Research, Czech Republic). The commercial graphene/PLA filament was extruded down the nozzle (Olsson Ruby-tipped 0.6 mm, 3DVerkstan, Sweden) at a temperature of 220 °C with a bed temperature of 60 °C. The 3D-printed electrodes were then activated to improve their conductivity by immersing in DMF for 4 h and rinsed with ethanol and water to remove the insulating PLA [13–16]. The electrodes were then dried in an oven at 65 °C for 2 h and used for dip-coating.

2.3. Dip-coating of 3D-printed nanocarbon electrodes

Initially, slurries of MXene ($Ti_3C_2T_x$) and the TMDs (MoS_2, $MoSe_2$, WS_2, and WSe_2) were prepared by adding 50 mg of the sample to 200 μL of DMF and bath sonicating for 30 min. The activated 3D-printed nanocarbon electrodes (3D-CEs) were then dipped into the respective slurry at room temperature for 3 h, as depicted in Scheme 1. The final electrodes were dried and subjected to morphological and electrochemical characterization. These dip-coated 3D-printed electrodes are referred to as $Ti_3C_2T_x$@3D-CE, MoS_2@3D-CE, $MoSe_2$@3D-CE, WS_2@3D-CE, and WSe_2@3D-CE in later sections.

2.4. Characterization

The surface morphology of the dip-coated activated 3D-printed nanocarbon electrodes was studied using SEM, TESCAN LYRA 3. The elemental composition and mapping were examined using an EDX detector (BRUKER XFlash 5010) attached to the SEM. The electrochemical measurements were carried out using a potentiostat (PGSTAT 204, Metrohm Autolab, Netherlands) operated by NOVA 2.1 software, where the dip-coated 3D-printed nanocarbon electrode (activated) was used as the working electrode (WE), with a platinum wire as the counter electrode (CE), and Ag/AgCl (1 M KCl) as the reference electrode (RE) in 0.5 M H_2SO_4 electrolyte. The specific current (mA/g) was calculated by dividing the current (mA) by the amount of active material (in grams) deposited on the electrode surface. The mass of the deposited material was calculated by measuring the mass of the nanocarbon electrodes before and after the dip-coating. All electrochemical measurements were carried out at ambient conditions in the open air and no other special conditions were used.

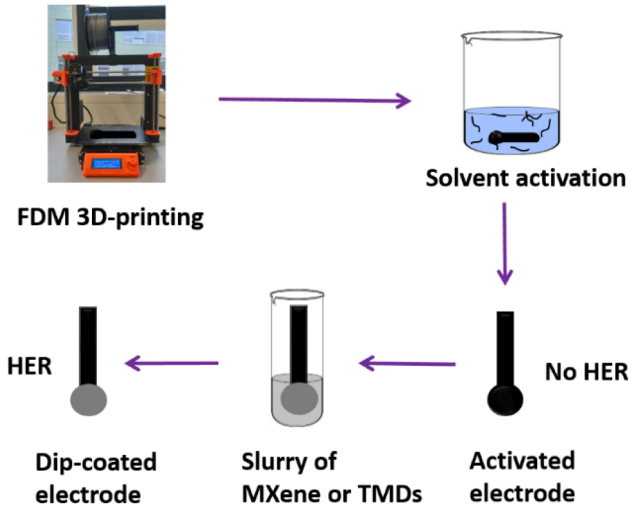

Scheme 1. Schematic representation of the dip-coating of activated 3D-printed nanocarbon electrode in a slurry of MXene or TMDs.

3. Results and discussion

The FDM technique was employed to fabricate a 3D-printed nanocarbon electrode using a commercial graphene/PLA filament followed by surface activation using DMF to improve the conductivity of the electrode surface [13,16,17,22]. The activated electrodes were then dip-coated in a slurry of layered materials as shown in Scheme 1.

A SEM image of the solvent-activated 3D-printed nanocarbon electrodes, which were subsequently used as substrates for dip coating, is shown in Fig. S1. The dip-coating method enables a binder-free coating of active materials to be achieved, due to the physisorption of layered materials on the surface of the 3D-printed electrode. An SEM micrograph and EDX spectrum of $Ti_3C_2T_x$@3D-CE are shown in Fig. 1A and B, respectively. It was found that the surface of the dip-coated 3D-printed nanocarbon electrode was attached with $Ti_3C_2T_x$ layers. . The EDX spectral analysis confirms the presence of titanium, carbon, oxygen, aluminum, fluorine, and chlorine with atomic percentages of 39.96, 23.65, 18.46, 9.57, 7.70, and 0.67%, respectively, over the surface of the dip-coated electrode (Fig. 1B). The presence of F and O on the electrode surface was ascribed to surface terminations (–F and –OH) from the processing of the original MAX phase to MXene [18–20]. The EDX mapping images shown in Fig. 1(C–H), further confirm the presence of the constituent elements Ti, C, O, F, Al, and Cl.

SEM micrographs of the dip-coated nanocarbon electrodes MoS_2@3D-CE, $MoSe_2$@3D-CE, WS_2@3D-CE, and WSe_2@3D-CE are shown in Fig. 2A–D, respectively. It was found that the microparticles are deposited on top of the electrode surfaces in each type of electrode. A

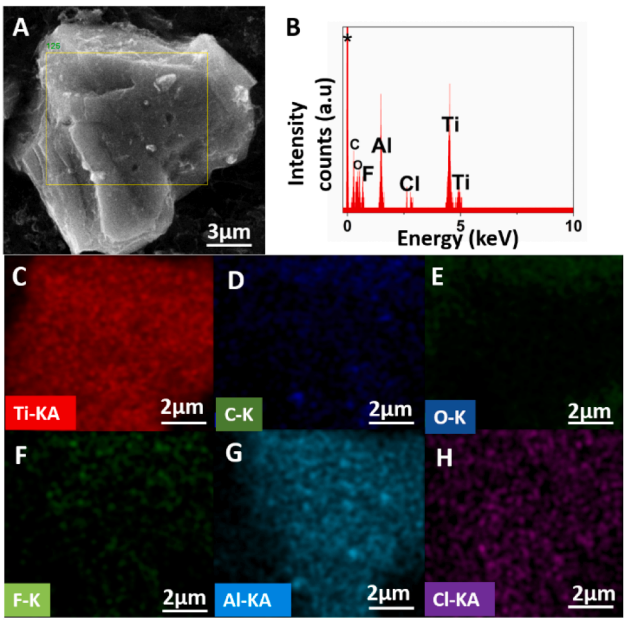

Fig. 1. (A) SEM, (B) EDX spectra of dip-coated MXene ($Ti_3C_2T_x$) on the 3D-printed nanocarbon electrode surface (* background peak), (C–H) EDX mapping of the individual elements Ti, C, O, F, Al, and Cl.

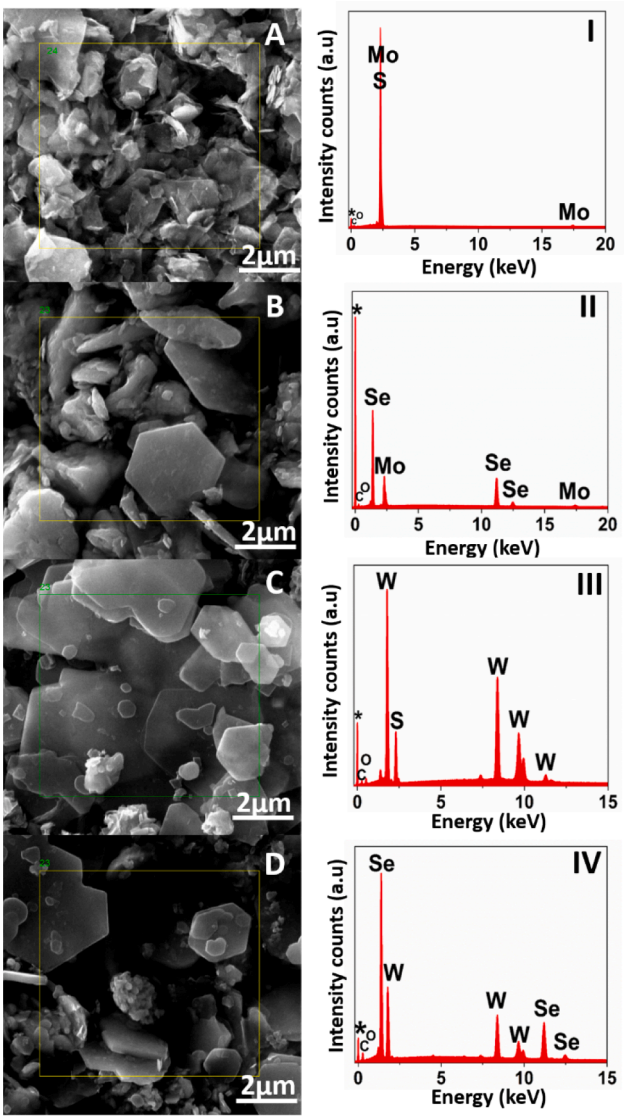

Fig. 2. SEM and EDX spectra of dip-coated electrodes (A, I) MoS_2@3D-CE; (B, II) $MoSe_2$@3D-CE; (C, III) WS_2@3D-CE; (D, IV) WSe_2@3D-CE; (* background peak).

spectral analysis was conducted to investigate the surface composition of the dip-coated nanocarbon electrodes using EDX spectroscopy for MoS_2@3D-CE, $MoSe_2$@3D-CE, WS_2@3D-CE, and WSe_2@3D-CE surfaces as depicted in Fig. 2I, II, III, and IV, respectively. The elemental compositions of the dip-coated electrodes are shown in Table S1.

Linear sweep voltammetry (LSV) was used to study the catalytic activity of the dip-coated 3D-printed nanocarbon electrodes through the hydrogen evolution reaction (HER) in acidic medium (0.5 M H_2SO_4), as shown in Fig. 3. The measurements were carried out in a potential range of 0 to −1.1 V at a scan rate of 5 mV s^{-1} to study the HER. The bare 3D-CE tends to be a poor catalyst for the HER, as shown in Fig. 3.

The activated dip-coated nanocarbon electrodes showed improved catalytic performance. It was found that for $Ti_3C_2T_x$@3D-CE, the potential required to attain a current density of −200 mA g^{-1} was −0.481 V. In the case of the TMD-based active catalysts, to reach −200 mA g^{-1} of current density the required potential was −0.620 and −0.496 V for MoS_2@3D-CE and $MoSe_2$@3D-CE, respectively, while for WS_2@3D-CE and WSe_2@3D-CE the required potential was −0.622 and −0.496 V, respectively. This demonstrates that dip-coating MXene ($Ti_3C_2T_x$) and TMD (MoS_2, $MoSe_2$, WS_2, and WSe_2) over 3D-CE modifies the electrode in such a way that it acts as an active catalyst material. The HER

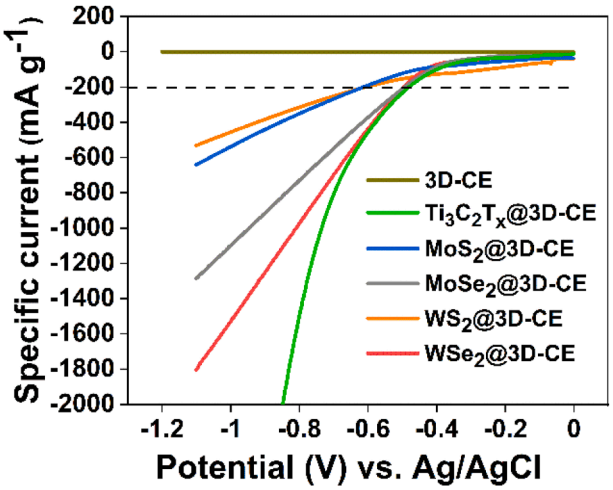

Fig. 3. LSV measurements using the various dip-coated electrodes.

measurements of the modified 3D-CEs were analyzed using the Tafel equation $\eta = b \log|j| + a$, where η is the overpotential, j is the specific current and b is the Tafel slope [21]. Tafel slopes determine rate-limiting steps of the HER measurements. The Tafel slope values were found to be 316 mV dec^{-1} for MXene@3D-CE and 335 and 260 mV dec^{-1} for $MoSe_2$@3D-CE and WSe_2@3D-CE, respectively. In the case of MoS_2@3D-CE and WS_2@3D-CE, very high Tafel slopes of 647 and 970 mV dec^{-1}, respectively, were attained (Fig. S2). In short, MXene-coated 3D-CE exhibits a low overpotential compared to the TMDs taken for analysis. Dip-coating of 3D-CEs with sulfide-based transition metals (MoS_2 and WS_2) produced high overpotentials and very high Tafel slope values when compared to the selenides of Mo and W. Furthermore, the stability of the electrodes was evaluated using the chronoamperometry measurement continuously for 2.5 h in 0.5 M H_2SO_4. Using the data obtained from the LSV measurement, a constant potential was applied to the electrodes based on the potential observed at the specific current of −200 mA g^{-1}. From the chronoamperometry measurement, the specific current versus time plot is drawn for all the electrodes up to 150 min, leaving an initial stability time of 5 min. (Fig. S3). The electrodes were found to be stable throughout the test while MoS_2@3D-CE showed some degradation which is in line with results previously reported by our group [10]. The small fluctuations in the specific current may be due to the detachment of H_2 gas from the surface of the electrode and not the materials themselves. The electrode performance is stable and the material is present on the electrode surface even after the electrochemical reactions, confirming a good affinity between the active material and the activated electrode (Fig. S4). This technique is shown to be a simple and scalable prototype method for catalytically activating the nanocarbon electrode surface using active layered and 2D materials for energy conversion purposes.

4. Conclusions

In summary, we have demonstrated a universal, fast, cost-effective approach for developing binder/surfactant-free modified 3D-printed electrodes for electrochemical applications. Dip-coating of activated 3D-printed nanocarbon electrodes in a slurry of titanium carbide (MXene) and transition metal dichalcogenides (TMDs) improved the catalytic property of the electrodes, as demonstrated for the hydrogen evolution reaction (HER). This method of fabricating a catalytically active 3D-printed nanocarbon electrode surface can be used to coat a variety of substrates, and may be adopted for various electrochemical applications in the future.

CRediT authorship contribution statement

K.P. Akshay Kumar: Investigation, Methodology, Formal analysis, Data curation, Validation, Writing - original draft. **Kalyan Ghosh:** Investigation, Writing - review & editing. **Osamah Alduhaish:** Funding acquisition. **Martin Pumera:** Conceptualization, Resources, Supervision, Writing - review & editing.

Declaration of Competing Interest

The authors declare that they have no known competing financial interests or personal relationships that could have appeared to influence the work reported in this paper.

Acknowledgment

This work was supported by the Distinguished Scientist Fellowship Program (DSFP) of King Saud University, Riyadh, Saudi Arabia.

Appendix A. Supplementary data

Supplementary data to this article can be found online at https://doi.org/10.1016/j.elecom.2020.106890.

References

[1] A. Ambrosi, M. Pumera, 3D-printing technologies for electrochemical applications, Chem. Soc. Rev. 45 (2016) 2740–2755, https://doi.org/10.1039/c5cs00714c.
[2] L.A. Verhoef, B.W. Budde, C. Chockalingam, B. García Nodar, A.J.M. van Wijk, The effect of additive manufacturing on global energy demand: an assessment using a bottom-up approach, Energy Policy 112 (2018) 349–360, https://doi.org/10.1016/j.enpol.2017.10.034.
[3] G.I.J. Salentijn, P.E. Oomen, M. Grajewski, E. Verpoorte, Fused deposition modeling 3D printing for (bio)analytical device fabrication: procedures, materials, and applications, Anal. Chem. 89 (2017) 7053–7061, https://doi.org/10.1021/acs.analchem.7b00828.
[4] M.R. Hartings, Z. Ahmed, Chemistry from 3D printed objects, Nat. Rev. Chem. 3 (2019) 305–314, https://doi.org/10.1038/s41570-019-0097-z.
[5] M.P. Browne, E. Redondo, M. Pumera, 3D-printing for electrochemical energy applications, Chem. Rev. 120 (2020) 2783–2810, https://doi.org/10.1021/acs.chemrev.9b00783.
[6] C. Zhu, T. Liu, F. Qian, W. Chen, S. Chandrasekaran, B. Yao, Y. Song, E.B. Duoss, J. D. Kuntz, C.M. Spadaccini, M.A. Worsley, Y. Li, 3D printed functional nanomaterials for electrochemical energy storage, Nano Today 15 (2017) 107–120, https://doi.org/10.1016/j.nantod.2017.06.007.
[7] P.L. dos Santos, S.J. Rowley-Neale, A.G.M. Ferrari, J.A. Bonacin, C.E. Banks, Ni−Fe (oxy)hydroxide modified graphene additive manufactured (3D-printed) electrochemical platforms as an efficient electrocatalyst for the oxygen evolution reaction, ChemElectroChem 6 (2019) 5633–5641, https://doi.org/10.1002/celc.201901541.
[8] M.P. Browne, J. Plutnar, A.M. Pourrahimi, Z. Sofer, M. Pumera, Atomic layer deposition as a general method turns any 3D-printed electrode into a desired catalyst: case study in photoelectrochemisty, Adv. Energy Mater. 9 (2019) 1–10, https://doi.org/10.1002/aenm.201900994.
[9] C. Iffelsberger, S. Ng, M. Pumera, Catalyst coating of 3D printed structures via electrochemical deposition: case of the transition metal chalcogenide MoS_x for hydrogen evolution reaction, Appl. Mater. Today 20 (2020), 100654, https://doi.org/10.1016/j.apmt.2020.100654.
[10] R. Gusmão, Z. Sofer, P. Marvan, M. Pumera, MoS_2 versatile spray-coating of 3D electrodes for the hydrogen evolution reaction, Nanoscale 11 (2019) 9888–9895, https://doi.org/10.1039/c9nr01876j.
[11] B. Cui, H. Lin, J.B. Li, X. Li, J. Yang, J. Tao, Core-ring structured $NiCo_2O_4$ nanoplatelets: synthesis, characterization, and electrocatalytic applications, Adv. Funct. Mater. 18 (2008) 1440–1447, https://doi.org/10.1002/adfm.200700982.
[12] Z. Ge, Z. He, An effective dipping method for coating activated carbon catalyst on the cathode electrodes of microbial fuel cells, RSC Adv. 5 (2015) 36933–36937, https://doi.org/10.1039/c5ra05543a.
[13] M.P. Browne, F. Novotný, Z. Sofer, M. Pumera, 3D printed graphene electrodes' electrochemical activation, ACS Appl. Mater. Interfaces 10 (2018) 40294–40301, https://doi.org/10.1021/acsami.8b14701.
[14] D.M. Wirth, M.J. Sheaff, J.V. Waldman, M.P. Symcox, H.D. Whitehead, J.D. Sharp, J.R. Doerfler, A.A. Lamar, G. Leblanc, Electrolysis activation of fused-filament-fabrication 3D-printed electrodes for electrochemical and spectroelectrochemical analysis, Anal. Chem. 91 (2019) 5553–5557, https://doi.org/10.1021/acs.analchem.9b01331.
[15] F. Novotný, V. Urbanová, J. Plutnar, M. Pumera, Preserving fine structure details and dramatically enhancing electron transfer rates in graphene 3D-printed electrodes via thermal annealing: toward nitroaromatic explosives sensing, ACS Appl. Mater. Interfaces 11 (2019) 35371–35375, https://doi.org/10.1021/acsami.9b06683.
[16] R. Gusmão, M.P. Browne, Z. Sofer, M. Pumera, The capacitance and electron transfer of 3D-printed graphene electrodes are dramatically influenced by the type of solvent used for pre-treatment, Electrochem. Commun. 102 (2019) 83–88, https://doi.org/10.1016/j.elecom.2019.04.004.
[17] C.L. Manzanares Palenzuela, F. Novotný, P. Krupička, Z. Sofer, M. Pumera, 3D-printed graphene/polylactic acid electrodes promise high sensitivity in electroanalysis, Anal. Chem. 90 (2018) 5753–5757, https://doi.org/10.1021/acs.analchem.8b00083.
[18] P. Srimuk, F. Kaasik, B. Krüner, A. Tolosa, S. Fleischmann, N. Jäckel, M.C. Tekeli, M. Aslan, M.E. Suss, V. Presser, MXene as a novel intercalation-type pseudocapacitive cathode and anode for capacitive deionization, J. Mater. Chem. A 4 (2016) 18265–18271, https://doi.org/10.1039/c6ta07833h.
[19] Y. Huang, H. Yang, Y. Zhang, Y. Zhang, Y. Wu, M. Tian, P. Chen, R. Trout, Y. Ma, T. H. Wu, Y. Wu, N. Liu, A safe and fast-charging lithium-ion battery anode using MXene supported Li_3VO_4, J. Mater. Chem. A 7 (2019) 11250–11256, https://doi.org/10.1039/c9ta02037c.
[20] N.M. Caffrey, Effect of mixed surface terminations on the structural and electrochemical properties of two-dimensional $Ti_3C_2T_2$ and V_2CT_2 MXenes multilayers, Nanoscale 10 (2018) 13520–13530, https://doi.org/10.1039/c8nr03221a.
[21] N.F. Rosli, M.Z.M. Nasir, N. Antonatos, Z. Sofer, A. Dash, J. Gonzalez-Julian, A. C. Fisher, R.D. Webster, M. Pumera, MAX and MAB phases: two-dimensional layered carbide and boride nanomaterials for electrochemical applications, ACS Appl. Nano Mater. (2019) 6010–6021, https://doi.org/10.1021/acsanm.9b01526.
[22] K.P. Akshay Kumar, Kalyan Ghosh, Osamah Alduhaish, Martin Pumera, Metal-plated 3D-printed electrode for electrochemical detection of carbohydrates, Electrochem. Commun. 120 (2020) 1–7, https://doi.org/10.1016/j.elecom.2020.106827, 106827.